(A) Western Blot of prostate cancer cell lines

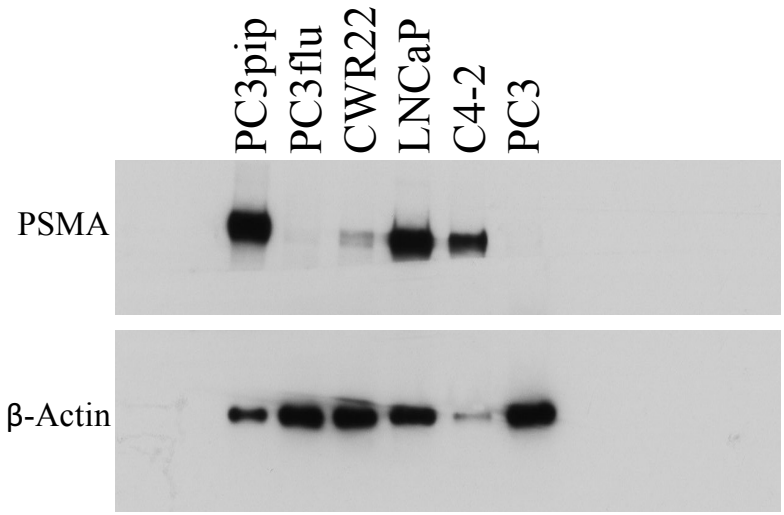

(B) Quantification of Western signals

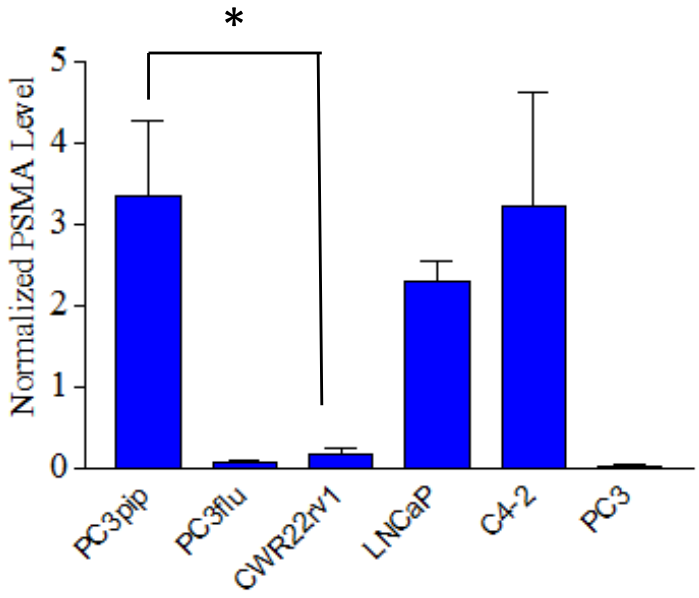

Figure S7: Expression of PSMA in prostate cancer cell lines. (A) Western blot analysis of PSMA expression in different prostate cancer cells lines. Cell lysate (20 µg protein) was resolved by 4-20% bis-acrylamide reducing SDS-PAGE and transferred to nitrocellulose. Membranes were blocked with 5% milk in TBST for 1 hour at room temperature. PSMA was detected with mAb J591 (1:2000) and β-Actin was detected anti-β-Actin (1:3000) (Sigma, A5441). Horseradish peroxidase-goat–anti-mouse IgG antibody (1:5,000 dilution) was used as 2nd antibody. Signals were quantified and PSMA signal normalized to β -actin signal. (B) Relative PSMA level in prostate cancer cell lines. PC3pip, LNCaP and C4-2 cells expressed similar level of PSMA. The amount of PSMA in CWR22rv1 cells was only 1/12 of that in PC3pip (*, p=0.029). Values are mean± SD of 3 replicates.

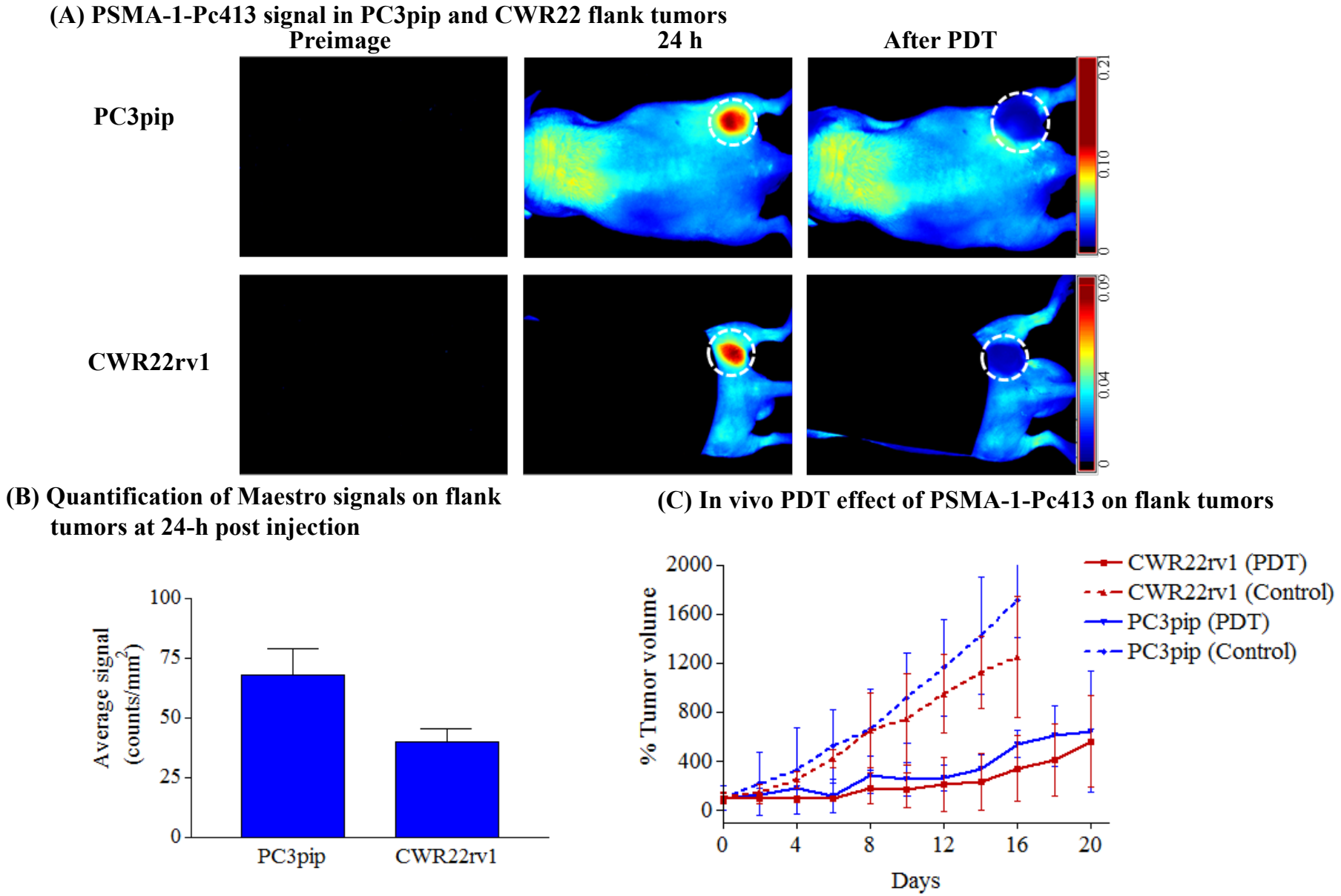

Figure S8: PDT treatment reduces CWR22rv1 tumor growth in flank tumors (no surgery). (A) Maestro images of mice receiving 0.5mg/kg PSMA-1-Pc413. At 24 hour post injection, selective accumulation of PSMA-1-Pc413 was observed in both PC3pip and CWR22rv1 tumors. After exposed to 150J/cm2 of 672nm laser, the signal was photo bleached, indicating photo activation of PSMA-1-Pc413. (B) Quantification of fluorescent signal in PC3pip and CWR22rv1 tumors 24h post injection. The fluorescent signal on CWR22rv1 tumor is about half of that on PC3pip tumors. (C) PDT was able to effectively inhibit both CWR22rv1 and Pc3pip tumor growth. Values are mean± SD of 4 animals.

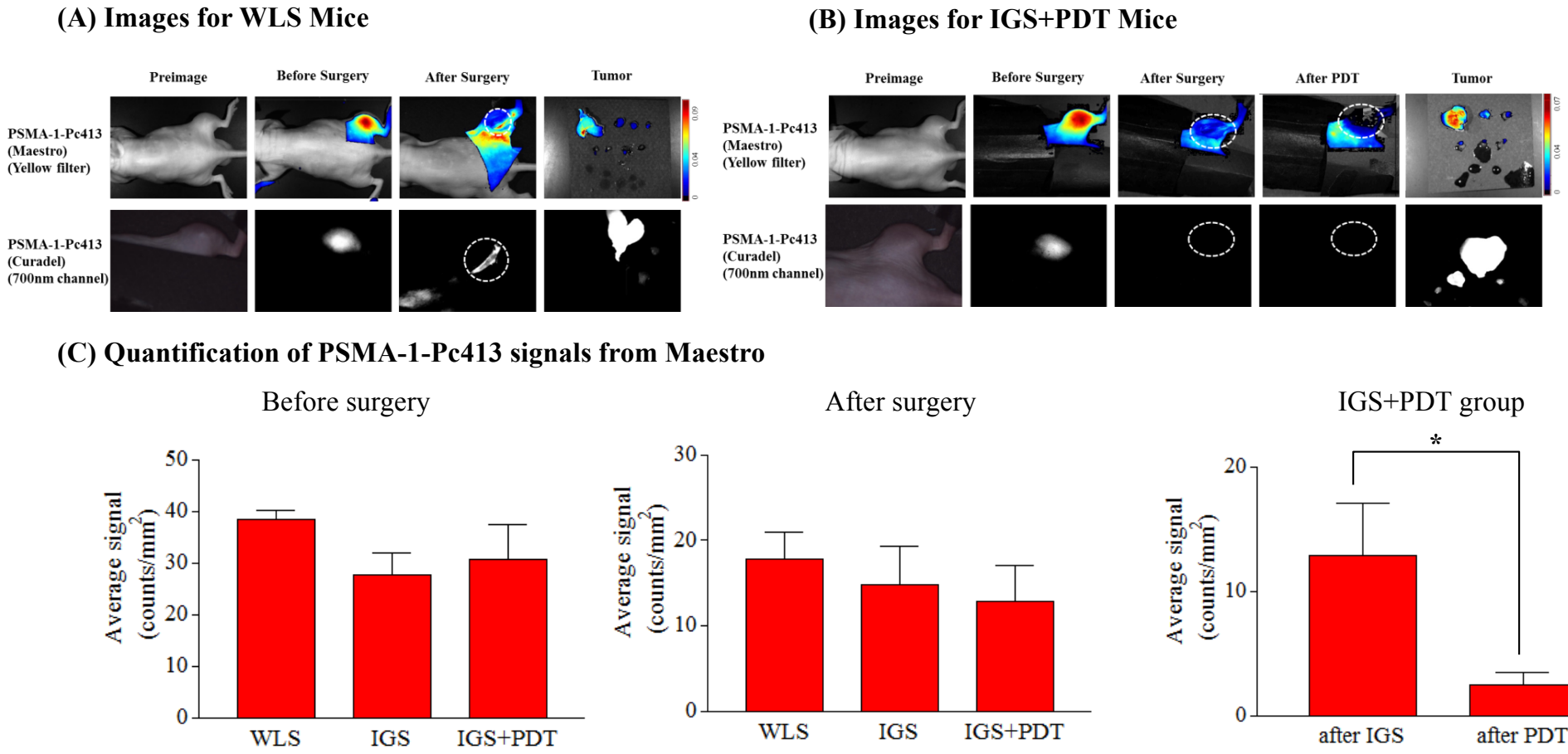

Figure S9: Use of PSMA-1-Pc413 for image-guided surgery followed by PDT treatment of CWR22rv1 intra-muscular tumors. (A) Representative images of WLS mice under Maestro and Curadel imaging systems. Circles indicate surgical bed. Residual PSMA-1-Pc413 signal were clearly seen in the wound, indicating presence of unresected tumor in the surgical wound. (B) Representative images of IGS+PDT mice under Maestro and Curadel imaging systems. Circles indicate surgical bed. Minimal amounts of PSMA-1-Pc413 signal was observed in the wounds after all surgeries, indicating tumor removal. After PDT, loss of PSMA-1-Pc413 was observed due to photo activation. (C) Quantification of PSMA-1-Pc413 signals in three experimental groups before surgery (left), after surgery (middle) and after IGS+PDT (right). Within the IGS+PDT group PDT further reduced PSMA-1-Pc413 signal significantly as compared to IGS alone (right) (*: p=0.000012). Values are mean±SD (n=5 for each group).

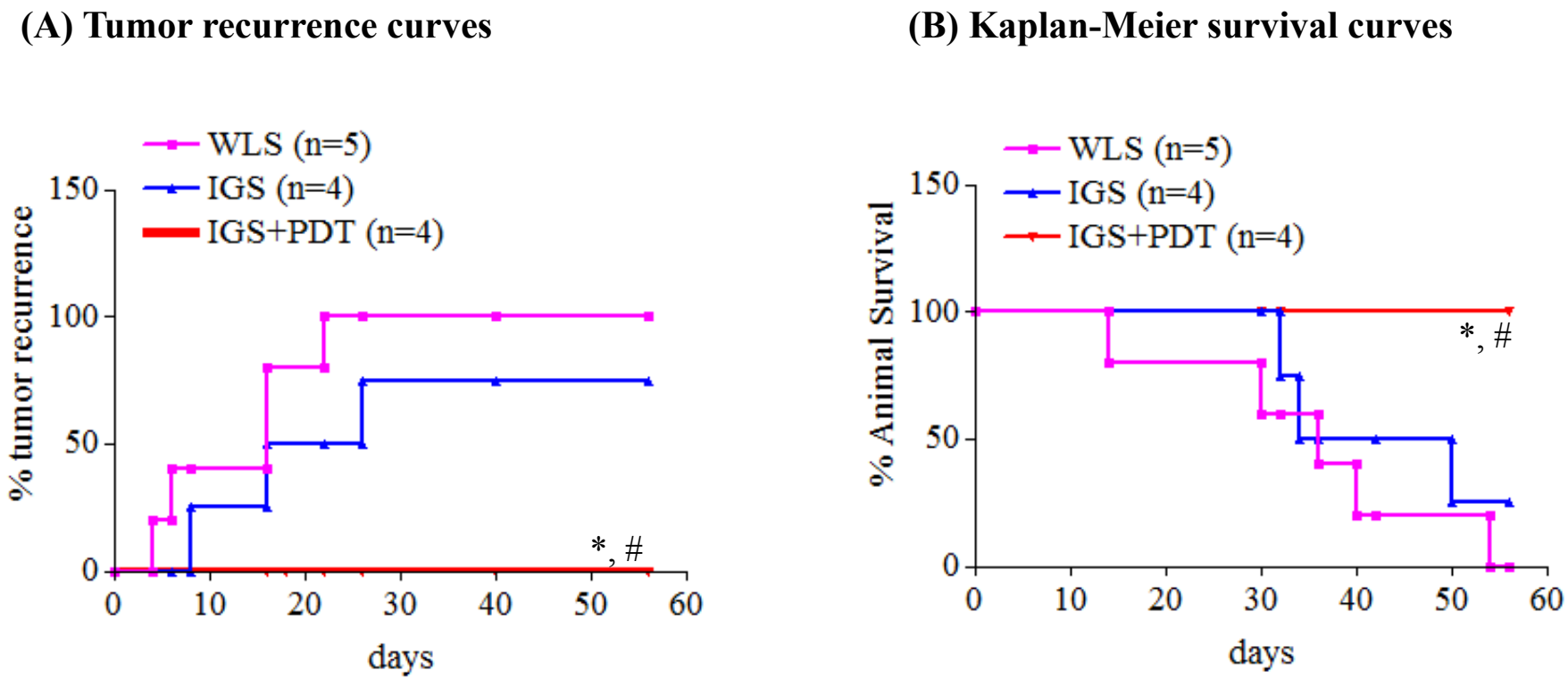

Figure S10: Combination of IGS and PDT delayed CWR22rv1 tumor recurrence and extended animal survival. (n=animal numbers). (A) Tumor recurrence curves of mice bearing CWR22rv1 tumor from three experimental groups. IGS did not significantly delay tumor recurrence as compared to WLS (p=0.5517). The tumor recurrence was significantly delayed by IGS+PDT (*: p=0.0020, IGS+PDT vs WLS; #: p=0.0068, IGS+PDT vs IGS). (C) Kaplan-Meier survival curves of mice from three experimental groups. IGS+PDT significantly prolonged animal survival (*: p=0.0001, IGS+PDT vs WLS; #: p=0.0126 IGS+PDT vs IGS).